Available online at www.sciencedirect.com
SCIENCE DIRECT®
Catalysis Today 85 (2003) 251–266
CATALYSIS TODAY
www.elsevier.com/locate/cattod

Conversion of N_2O to N_2 on TiO_2(1 1 0)

Michael A. Henderson*, Janos Szanyi, Charles H.F. Peden

Environmental Molecular Sciences Laboratory, Pacific Northwest National Laboratory, P.O. Box 999, MS K8-93, Richland, WA 99352, USA

Received 11 February 2003; received in revised form 27 March 2003; accepted 28 March 2003

Abstract

In this study, we examine the interaction of N_2O with TiO_2(1 1 0) in an effort to better understand the conversion of NO_x species to N_2 over TiO_2-based catalysts. The TiO_2(1 1 0) surface was chosen as a model system because this material is commonly used as a support and because oxygen vacancies on this surface are perhaps the best available models for the role of electronic defects in catalysis. Annealing TiO_2(1 1 0) in vacuum at high temperature (above about 800 K) generates oxygen vacancy sites that are associated with reduced surface cations (Ti^{3+} sites) and that are easily quantified using temperature programmed desorption (TPD) of water. Using TPD, X-ray photoelectron spectroscopy (XPS) and electron energy loss spectroscopy (EELS), we found that the majority of N_2O molecules adsorbed at 90 K on TiO_2(1 1 0) are weakly held and desorb from the surface at 130 K. However, a small fraction of the N_2O molecules exposed to TiO_2(1 1 0) at 90 K decompose to N_2 via one of two channels, both of which are vacancy-mediated. One channel occurs at 90 K, and results in N_2 ejection from the surface and vacancy oxidation. We propose that this channel involves N_2O molecules bound at vacancies with the O-end of the molecule in the vacancy. The second channel results from an adsorbed state of N_2O that decomposes at 170 K to liberate N_2 in the gas phase and deposit oxygen adatoms at non-defect Ti^{4+} sites. The presence of these O adatoms is clearly evident in subsequent water TPD measurements. We propose that this channel involves N_2O molecules that are bound at vacancies with the N-end of the molecule in the vacancy, which permits the O-end of the molecule to interact with an adjacent Ti^{4+} site. The partitioning between these two channels is roughly 1:1 for adsorption at 90 K, but neither is observed to occur for moderate N_2O exposures at temperatures above 200 K. EELS data indicate that vacancies readily transfer charge to N_2O at 90 K, and this charge transfer facilitates N_2O decomposition. Based on these results, it appears that the decomposition of N_2O to N_2 requires trapping of the molecule at vacancies and that the lifetime of the N_2O–vacancy interaction may be key to the conversion of N_2O to N_2.

Keywords: TiO_2(1 1 0); Vacancy oxidation; N_2O; N_2; Temperature programmed desorption; X-ray photoelectron spectroscopy; Electron energy loss spectroscopy

1. Introduction

Processes that convert NO_x species to di-nitrogen are of immense importance and interest to the fields of heterogeneous catalysis and environmental science. NO_x species are typically generated in hydrocarbon combustion processes in air, and their emission has significant environmental consequences in the form of acid rain and greenhouse warming. There is therefore a general need for catalysts that efficiently convert NO_x species to N_2. Noble-metals supported on oxides have been shown to be effective catalysts for the conversion of N_2O to N_2 (for example, see recent work by Christoforou et al. [1]), however, the role of

* Corresponding author. Tel.: +1-509-3762192; fax: +1-509-3765106.
E-mail address: ma.henderson@pnl.gov (M.A. Henderson).

0920-5861/$ – see front matter © 2003 Elsevier B.V. All rights reserved.
doi:10.1016/S0920-5861(03)00392-4

the oxide is not well understood. Reducible oxides, such as TiO_2 [2–4], CeO_2 [5] and Fe_2O_3 [6] have been shown to convert N_2O to N_2 presumably at oxygen vacancy sites. N_2O has also been observed to behave as an electron scavenger in photocatalysis over TiO_2 [7–9]. In terms of thermal N_2O decomposition activity on TiO_2, the rutile phase has been shown to be more active than the anatase phase [10]. Studies on the chemical properties of oxygen vacancies on the rutile TiO_2(1 1 0) surface are numerous [11], providing an excellent model system for study of NO_x–vacancy interactions.

N_2O is the major product from the thermal or photochemical decomposition of NO on TiO_2 [12–18] indicating that N–N bond formation is feasible. However, full conversion of NO to N_2 over TiO_2 surfaces is difficult, suggesting that N_2O activation is a 'bottleneck' in the conversion of NO to N_2. In this study, we examine the conversion of N_2O to N_2 over the model catalyst oxide support, namely rutile TiO_2(1 1 0). We find that N_2 is produced from two distinct channels of N_2O chemistry, but that the overall yield of N_2 is limited by the surface vacancy population and by the adsorption temperature.

2. Experimental

Experiments described in this work were performed in two separate ultrahigh vacuum (UHV) chambers [19,20] using a TiO_2(1 1 0) crystal obtained from First Reaction. The crystal was mounted using a tantalum backing plate as described elsewhere [20], and was cleaned in UHV by sputter/anneal cycles. After cleaning, no features were observed in Auger electron spectroscopy (AES) or X-ray photoelectron spectroscopy (XPS) other than those associated with Ti and O, and a sharp 1×1 low-energy electron diffraction (LEED) pattern was typically observed. Reagents (N_2O, O_2, and H_2O) used in this study were all of research-grade purity. As received, the N_2O source contained significant amounts of N_2 and NO. These impurities were removed using freeze-pump thaw cycles with liquid nitrogen (LN2). While N_2 was not condensed by the LN2 trap, and thus was easily removed, the NO impurity was separated by pumping off the first component of the condensed gas to escape the LN2 trap after the LN2 was removed. Water was also further purified using freeze–pump–thaw cycles prior to use, and O_2 was passed through an LN2 trap prior to use. Dedicated gaslines were conditioned to each molecule by prolonged exposure to Torr pressures prior to use. No apparent decomposition of N_2O was detected in the gas handling system after prolonged exposure of the gas in the gasline.

TPD was performed using a line-of-sight quadrupole mass spectrometer (QMS) and a heating rate of 2 K/s. For each TPD experiment, unless otherwise indicated, the TiO_2(1 1 0) crystal was annealed in UHV at 850 K for 10 min, then cooled in UHV to the desired adsorption temperature. This procedure generated a surface possessing a low coverage of oxygen vacancy sites that could be determined using water TPD [21]. Gases were typically dosed using a calibrated collimated doser that preferentially exposed the TiO_2(1 1 0) surface, but not the sample holder.

3. Results

3.1. TPD results

Fig. 1 shows N_2O TPD spectra ($m/e = 44$) for various exposures of N_2O on TiO_2(1 1 0) at 90 K. For each experiment, a fresh surface was prepared by annealing (see Section 2) to generate an oxygen vacancy population of about 14% (7×10^{13} cm^{-2}). At the lowest N_2O exposure (6×10^{13} molecules/cm^2), two N_2O TPD peaks were observed at 170 and 145 K. TPD of higher exposures showed that the 170 K N_2O TPD peak was nearly saturated at the lowest exposure employed, whereas the 145 K peak increased in peak area and shifted to 130 K. A third N_2O TPD peak developed for exposures above about 5×10^{14} molecules/cm^2. Although this third peak also grew with increasing exposure, its peak area was limited by the fact that its leading edge coincided with the adsorption temperature employed in these studies. Based on comparisons with other N_2O surface studies in the literature [22,23], we assign the 100 K N_2O TPD peak to desorption of multilayer N_2O.

Although the data presented in Fig. 1 is limited to temperatures up to 220 K, the TPD ramp was extended in each experiment up to 600 K. No desorption products were detected above 200 K. Aside from the $m/e = 44$ signals shown in Fig. 1, traces

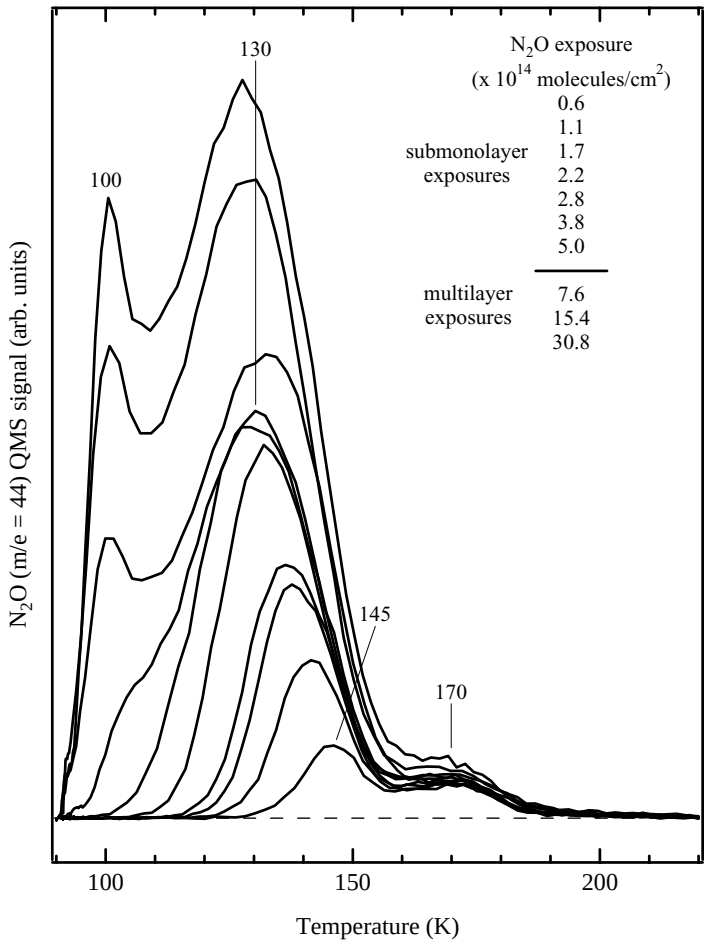

Fig. 1. N_2O TPD spectra ($m/e = 44$) from various exposures of N_2O dosed on $TiO_2(1\,1\,0)$ at 90 K. The surface was annealed at 850 K prior to N_2O adsorption, and possessed about 14% oxygen vacancy sites.

corresponding to the other QMS cracking fragments of N_2O ($m/e = 14$, 28 and 30) were also followed, as shown in Fig. 2. The $m/e = 14$, 28 and 30 traces generally tracked the signal of the parent molecule at $m/e = 44$, particularly in the 130 K TPD peak. The ratios of these signals to that of the parent matched the QMS cracking ratios of N_2O obtained from backfilling the chamber. However, the $m/e = 28$ to 44 ratio was greater in the 170 K peak, with a value of about 1, compared a value of about two thirds obtained from the 130 K peak. Analysis of the $m/e = 16$ signal (not shown) indicated that the enhancement in the $m/e = 28$ signal at 170 K was not due to contributions from CO or CO_2 adsorbed from background, despite the fact that both of these species desorb from $TiO_2(1\,1\,0)$ below 200 K [24,25]. Also, TPD after exposure of the crystal to background indicated that CO, CO_2 or N_2 were not adsorbed in detectable amounts during the time period between typical TPD experiments. The enhancement in the $m/e = 28$ signal at 170 K therefore likely resulted from an N_2O-related N_2 desorption peak located coincident with the 170 K N_2O TPD state.

A gauge of the uptake of N_2O on $TiO_2(1\,1\,0)$ can be had by plotting the N_2O TPD peak area from the data in Fig. 1 as a function of N_2O exposure. This plot, shown in Fig. 3, indicates that the amount of N_2O evolved in TPD was linearly related to exposure

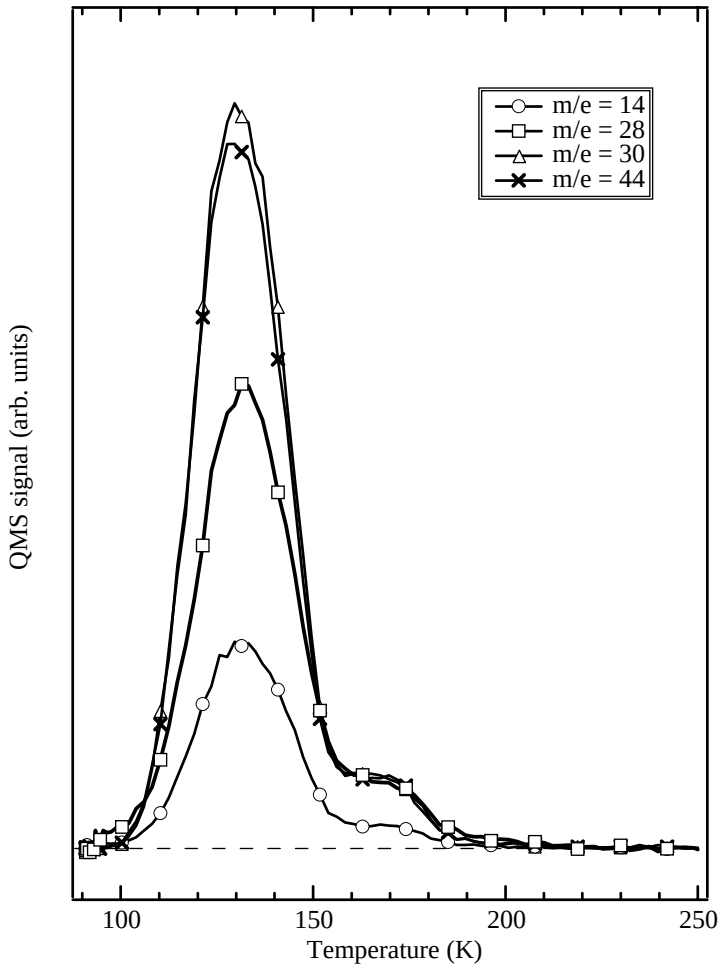

Fig. 2. TPD traces from the parent N_2O ($m/e = 44$) and from the QMS cracking fragments NO ($m/e = 30$), N_2 ($m/e = 28$) and N ($m/e = 14$) for a monolayer coverage of N_2O adsorbed on $TiO_2(1\,1\,0)$ at 90 K.

in the low exposure regime. The linear yield of N_2O in TPD continued to about the monolayer saturation point, above which the TPD yield approached a saturation with respect to increasing exposure. The inset illustrates that the linear-dependent regime at low exposure passed through the origin implying little or no irreversible decomposition of N_2O on $TiO_2(1\,1\,0)$. Based on these data, one might conclude that N_2O does not decompose on $TiO_2(1\,1\,0)$, and that the saturation of the TPD yield for high exposures was due to a decreased sticking coefficient owing the proximity of the adsorption temperature (90 K) to the leading edge of the multilayer TPD state.

Data in Fig. 4 verifies that the sticking probability of N_2O on $TiO_2(1\,1\,0)$ at 90 K is coverage-dependent, but also suggests that some decomposition of N_2O occurred on adsorption at 90 K. Fig. 4 corresponds to a King and Wells [26] experiment in which the sample was positioned ~1 mm in front of the doser tube, and the QMS was used to track the extent to which the crystal adsorbed N_2O. Although only $m/e = 28$ and 44 are shown in the figure, traces for the other cracking fragments of N_2O tracked that of the $m/e = 44$ signal. The bold traces correspond to exposure of a 8.5×10^{12} molecules/cm^2 s N_2O flux to the $TiO_2(1\,1\,0)$ crystal at 90 K, whereas the fine traces ('filled in' to the

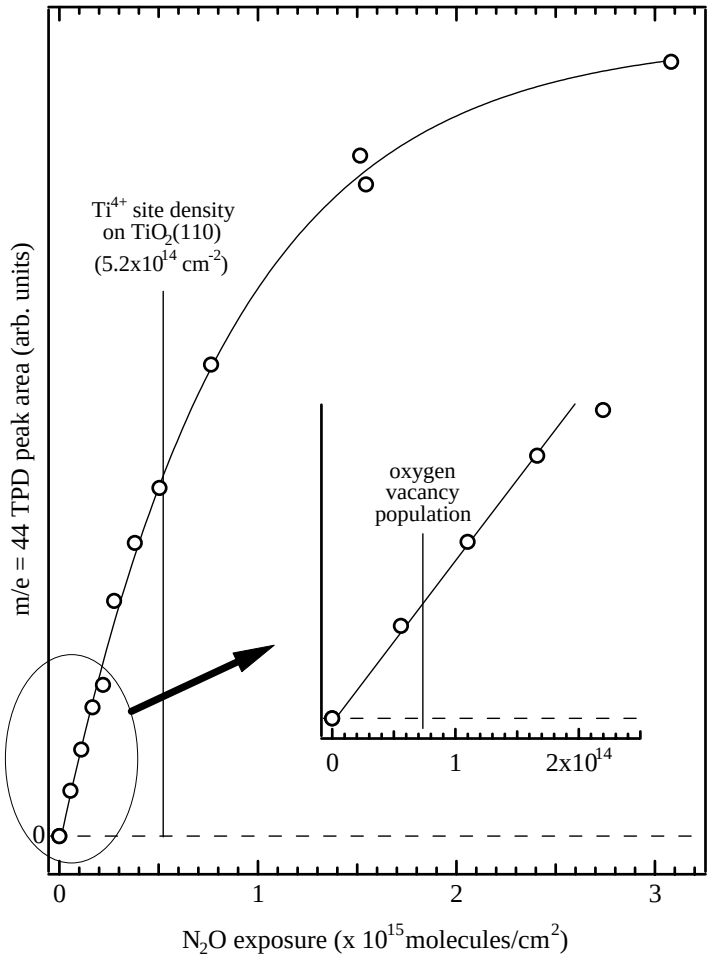

Fig. 3. N_2O TPD peak area as a function of N_2O exposure on $TiO_2(1\,1\,0)$ at 90 K. The data were taken from the N_2O TPD traces shown in Fig. 1. The inset shows a magnification of the low exposure regime. The curve through the data is drawn to guide the eye.

level of the bold traces) are for the same N_2O flux exposed to a stainless steel flag at RT. The 'square wave' pattern of the 'stainless steel' traces implies that little or no adsorption occurred on the flag, thus permitting these traces to be used to gauge the extent of N_2O sticking on $TiO_2(1\,1\,0)$ at 90 K. In the monolayer exposure regime, the initial sticking coefficient of N_2O on $TiO_2(1\,1\,0)$ at 90 K was near unity (about 0.95) as gauged by the $m/e = 44$ signal, but decreased rapidly for exposures above about 5×10^{14} molecules/cm^2. The surface appeared saturated by an exposure of about 2×10^{15} molecules/cm^2. However, it is clear from the 'pumping' tail after termination of the N_2O flux (the point labeled 'dose end') that N_2O adsorption and desorption were both occurring at 90 K in the high exposure regime. We assign the slow evolution of N_2O after termination of the dose to desorption of multilayer N_2O owing to the proximity in temperature of the leading edge of the multilayer state to the adsorption temperature (see Fig. 1).

Although the $m/e = 28$ QMS signal generally followed that of the parent signal, the lower traces in Fig. 4 indicate that a small 'burst' of N_2 was detected during the initial N_2O exposure regime at 90 K. The $m/e = 14$ signal (not shown) also registered a small 'burst', indicating that the $m/e = 28$ signal was

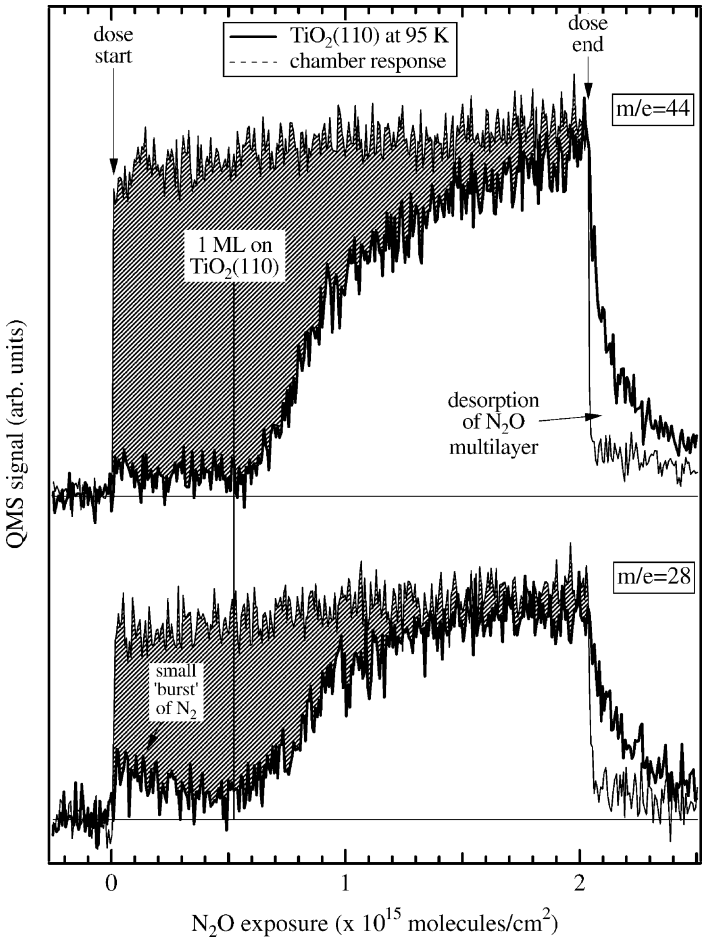

Fig. 4. King and Wells [26] uptake measurement using the $m/e = 44$ (upper, displaced vertically for clarity) and $m/e = 28$ (lower) QMS signals for N_2O exposed to $TiO_2(1\,1\,0)$ at 90 K. The bold traces are for N_2O exposed to the $TiO_2(1\,1\,0)$ surface, and the fine traces are for N_2O exposed to a stainless steel flag at RT. The areas indicated by the filled-in regions between the traces corresponds to the uptake of N_2O by the $TiO_2(1\,1\,0)$ crystal. The N_2O flux for each experiment ($TiO_2(1\,1\,0)$ and flag) was about 8.4×10^{12} molecules/cm^2 s.

not due to displacement of CO adsorbed from background, but from N_2 evolved by N_2O decomposition. We can also exclude the possibility that this signal arose from adsorption and desorption of trace amounts of N_2 in the N_2O source for two reasons. First, as mentioned in the experimental section, it was relatively straightforward to remove N_2 from the N_2O source using freeze–pump–thaw cycles in LN2. Second, although the onset of the N_2 'burst' coincided with the start of the dose, it attenuated in a manner consistent with 'consumption' of some reactive surface site. Based on these observations, we conclude that trace levels of N_2O decomposed during the initial exposure to $TiO_2(1\,1\,0)$ at 90 K resulting in ejection of N_2 into vacuum. No other desorption products (e.g., NO or O_2) were observed. The ejection of N_2 into vacuum during N_2O adsorption at low temperature (<100 K) has been seen on metal [23,27] and oxide [5] surfaces. The ejection of N_2 without coincident detection of O_2 or NO suggests that oxygen in some form was left on the surface.

An estimate of the amount of N_2 desorbed during N_2O exposure at 90 K was obtained using the King and Wells data shown in Fig. 4 by scaling the $m/e = 28$ signals to that of the $m/e = 44$ signals. Using this procedure, we estimate that the area between the solid and

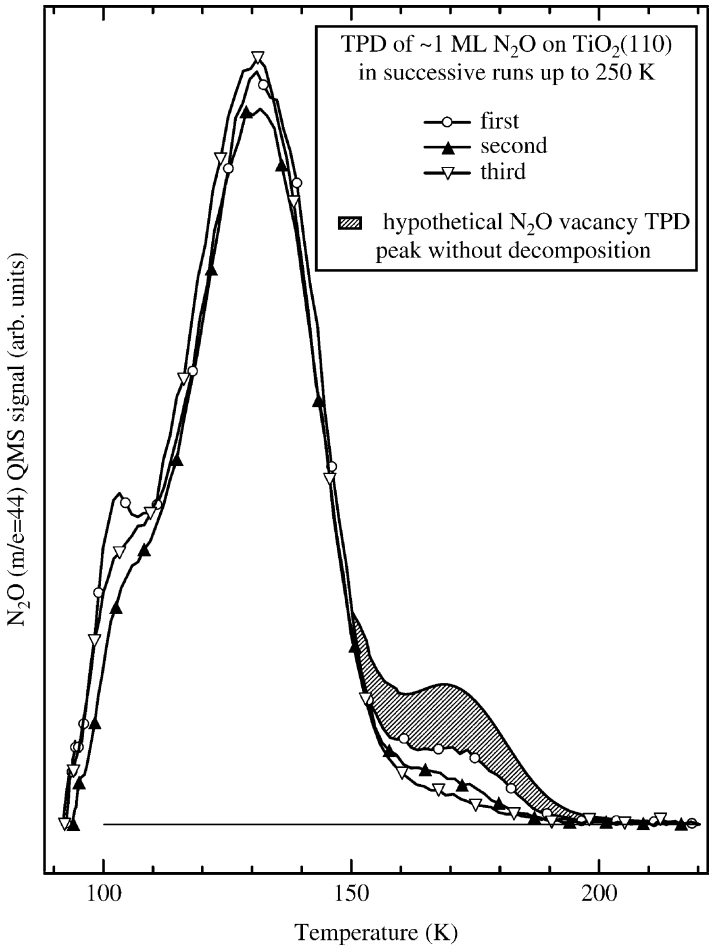

Fig. 5. N_2O TPD spectra ($m/e = 44$) for successive TPD experiments terminated at 250 K. The N_2O coverage in each was equal to or slightly greater than monolayer saturation. The trace filled in to the level of the first TPD experiment represents what hypothetically might be expected if no N_2O decomposition were to occur in the first TPD experiment.

dashed traces in the exposure regime below the 1 ML point was about 10% smaller for the scaled $m/e = 28$ signals compared to that obtained using the $m/e = 44$ signals. Assuming that the $m/e = 28$ QMS signal from ionization of N_2 is similar to that of the $m/e = 28$ QMS signal from ionization of N_2O, we estimate that the amount of N_2 evolved during exposure of N_2O to TiO_2(1 1 0) at 90 K was no greater than about 0.1 ML. The fact that the TPD uptake measurement of Fig. 3 does not register a consumption of N_2O suggests that at 90 K the ratio of the amount decomposed versus the amount adsorbed is coverage-independent in the low coverage regime, with the latter favored over the former. This is partially supported by the fact that while the N_2 burst attenuated from the start of the dose, as shown in Fig. 4, it extended to nearly saturation of the monolayer.

An alternative approach using N_2O TPD provides additional verification of trace N_2O decomposition, as well as a better estimate of the amount of N_2O decomposition. Fig. 5 shows N_2O TPD spectra from successive TPD runs in which the maximum temperature for the end point of each run was restricted to 250 K. Unlike for the TPD data in Fig. 1, in which the surface was regenerated to its original condition prior to the next N_2O TPD experiment, the maximum tem-

perature restriction of 250 K tests the extent to which the surface has been modified by N_2O. In these experiments, an exposure of N_2O equivalent to monolayer saturation was used. The first N_2O TPD experiment (circular markers) is consistent with a similar exposure in Fig. 1. In the second and third runs, the main N_2O TPD peak at 130 K was relatively unchanged (although the exposure of N_2O in each case was slightly different as evidenced by changes in the multilayer shoulder at 100 K). However, the amount of N_2O detected in the 170 K TPD peak decreased by about 50% for each successive run. This observation suggests that the amount of N_2O in the 170 K TPD peak for the first TPD run may have been only 50% of that expected if no decomposition occurred. In fact, the peak area of the 170 K N_2O state for the first run is about 7% of the peak area in the 130 K N_2O TPD state, which the data in Fig. 4 indicate corresponded roughly to 1 ML of N_2O. Given that the surface possessed 14% vacancy sites (based on water TPD; see below). The fine trace in Fig. 5 represents what might be expected for the 170 K N_2O TPD peak if no N_2O decomposition had occurred. It appears that about half of the sites responsible for the 170 K TPD state were modified and half remained active for subsequent encounters with N_2O molecules. This 1:1 ratio of desorption (reactive site unchanged) to decomposition (reactive site modified) continued in successive TPD runs when the maximum temperature was limited to 250 K.

The TPD data of Fig. 5 shows that N_2O modifies the $TiO_2(1\,1\,0)$ surface. The nature of this modification is difficult to discern from the data of Fig. 5, although one may assume that vacancy sites are being oxidized based on the work of Shultz et al. [28] who previously observed defect oxidation by O_2 and N_2O. The modification of $TiO_2(1\,1\,0)$ by N_2O can be characterized using a probe molecule such as water. Water is sensitive to the presence of oxygen vacancies and other structural anomalies on $TiO_2(1\,1\,0)$ [29]. Fig. 6 shows H_2O ($m/e = 18$) TPD spectra after various surface pretreatments with N_2O or O_2. In each case, the response of H_2O to the N_2O/O_2 modified surface was compared to the H_2O TPD spectrum from the clean surface possessing 14% oxygen vacancy sites (fine line traces). In Fig. 6A (bottom), approximately 1 ML of water was adsorbed at 90 K on $TiO_2(1\,1\,0)$ after the surface had been exposed to a monolayer saturation exposure of N_2O at 90 K that was then preheated to 250 K. The H_2O TPD traces with and without this N_2O pretreatment are different in two ways. First, the amount of H_2O that desorbed in the 500 K TPD peak was about 50% less for the case of the N_2O pretreated surface. The 500 K H_2O TPD peak is due to recombinative desorption of water molecules dissociatively adsorbed at oxygen vacancy sites, and provides an accurate measure of the vacancy coverage on the surface [29]. The 50% reduction in the 500 K TPD peak area suggests that a single N_2O TPD pretreatment oxidized 50% of the oxygen vacancy sites, in agreement with the data in Fig. 5. We may therefore reasonably conclude, based on a comparison of the TPD data in Figs. 5 and 6, that the 170 K N_2O TPD state is due to N_2O molecules desorbing from vacancy sites. Second, there was also a change in the trailing edge of the 270 K H_2O TPD peak as a result of the N_2O pretreatment. Previous studies have shown that the 270 K H_2O TPD peak is due to desorption of molecularly adsorbed water [20,30,31], but that the development of new states on the trailing edge of this peak result from recombinative desorption of dissociated water [32]. For example, data shown in Fig. 6B illustrate that O_2 pretreatment oxidized the oxygen vacancies (no 500 K H_2O TPD state) and resulted in a new TPD feature on the trailing edge of the 270 K H_2O TPD peak. The shaded area in the plots of Fig. 6A and B indicates that roughly twice as much water desorbed in the new H_2O TPD state at RT as a result of O_2 pretreatment as compared to the case of N_2O pretreatment. We have previously shown that this new water desorption feature, occurring at about RT, results from the influence of oxygen adatoms deposited on the $TiO_2(1\,1\,0)$ cation rows coincident with the oxidation (filling) of oxygen vacancy sites [32,33]. That is, one oxygen atom from the O_2 molecule reacts with the vacancy while the other resides at a Ti^{4+} site as an adatom. In fact, Schaub et al. [34] have detected O adatom species on $TiO_2(1\,1\,0)$ using STM. These authors have shown that O adatom species exhibit the ability to diffuse along the rows of Ti^{4+} sites and to transfer vacancies laterally from row to row of bridging O^{2-} sites. The O adatoms also readily abstract protons from N–H or O–H bonds to produce in terminal OH groups at Ti^{4+} sites [32,35].

The data in Fig. 6A suggest that during a typical N_2O TPD experiment (adsorption at 90 K) approximately half of the oxygen vacancy sites were oxidized and about half as many O adatoms were deposited

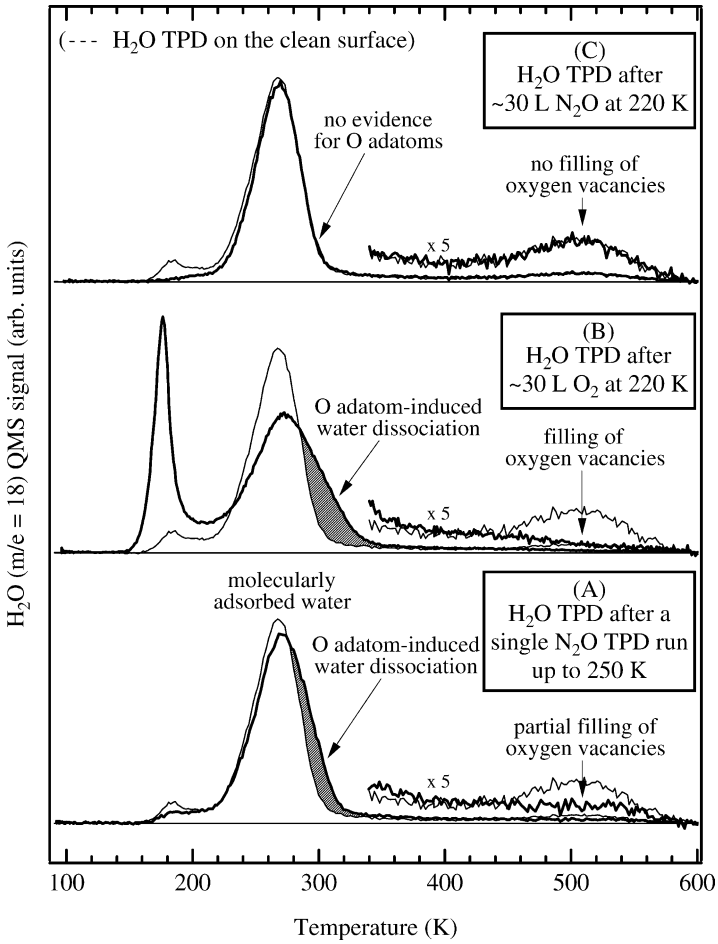

Fig. 6. H_2O TPD ($m/e = 18$) spectra probing the influence of N_2O (A and C) and O_2 (B) adsorption on the surface of $TiO_2(1\,1\,0)$. Spectra are displaced vertically for clarity, and each is compared to the spectrum of H_2O dosed on the clean surface (fine line traces). In each case, the H_2O coverage was equal to or slightly greater than that of monolayer saturation.

on the surface as compared to the case in which the surface was pretreated with O_2 (Fig. 6B). In concept, one might argue that N adatoms could be deposited by cleaving the N=NO bond and that these N adatoms might behave toward water in a similar manner as the O adatoms studied previously [32,35]. However, this does not take place based on our XPS results (see below) that show little or no N left on the surface above 180 K. Dissociation of the N=NO bond is less likely to occur than dissociation of the NN=O bond because the gas phase bond dissociation energy of the former is nearly three times that of the latter [36].

The chemistries of O adatom deposition and vacancy oxidation from N_2O differ from those of O_2 not only in extent, but also in temperature dependence. Whereas Fig. 6B shows that both O adatom deposition and vacancy oxidation occurred for O_2 adsorption at 220 K, Fig. 6C shows this was not the case for N_2O adsorption at 220 K. As opposed to the conditions of the experiment in Fig. 6A in which N_2O was adsorbed at 90 K, a 30 L N_2O exposure at 220 K resulted in no detectable affect on water. The H_2O TPD profiles with and without N_2O treatment at 220 K were virtually identical. In other words, no reactive sticking was observed for a 30 L N_2O exposure to $TiO_2(1\,1\,0)$ at 220 K. We have previously shown that the reactive sticking of O_2 at oxygen vacancies is also temperature-dependent between 100 and 200 K

[33], however, the data in Fig. 6B clearly show that a 30 L exposure of O_2 at 220 K oxidizes the vacancies whereas this is not the case for N_2O. This result is in contrast with findings by Shultz et al. [28] who concluded based on XPS results that the abilities of O_2 and N_2O to oxidize electronic defects on TiO_2(1 1 0) at RT were approximately equivalent.

A maximum reactive sticking probability for N_2O at 220 K can be estimated assuming a sensitivity level for H_2O in TPD of 0.01 ML. The absence of a change in the 500 K H_2O TPD peak after a 30 L N_2O exposure suggests that the reactive sticking of N_2O at 220 K is $\leq 5\times10^{-4}$. In the case of N_2O, the reactivity appears to depend on occupation of a low temperature adsorption state whose lifetime at 220 K (under UHV conditions) is too short to permit decomposition and oxidation of vacancies. A similar temperature-dependence in the reactive sticking of N_2O was observed by Haq and Hodgson [23] for the Pd(1 1 0) surface. This temperature dependence in the reactive sticking of N_2O might be overcome at higher N_2O exposure pressures wherein a high steady-state coverage of N_2O can be maintained at higher temperature.

3.2. XPS results

XPS measurements were used to follow the interaction of N_2O with TiO_2(1 1 0). Fig. 7 shows the N 1s

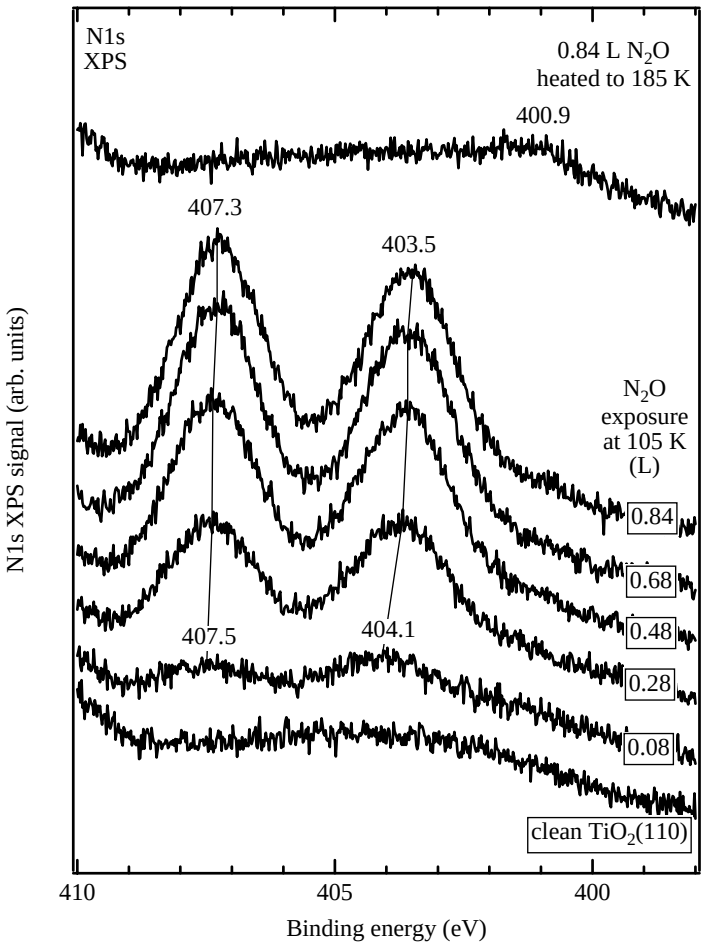

Fig. 7. N 1s XPS spectra from clean TiO_2(1 1 0) (lower trace), from increasing exposures of N_2O at 105 K (middle traces) and from a 0.84 L exposure at 105 K heated to 185 K (upper trace). Spectra are displaced vertically for clarity.

XPS spectrum for various exposures of N_2O adsorbed on TiO_2(1 1 0) at 105 K. This adsorption temperature was the lowest achievable in the XPS chamber, which precluded formation of a saturated N_2O monolayer based on the TPD data of Fig. 1. At the lowest exposure, 0.08 L, two N 1s features of equivalent intensity at 404.1 and 407.5 eV are indicative of N_2O. The lower BE feature arises from the N atom at the end of the molecule [5]. These features shifted down in binding energy (BE) to 403.5 and 407.3 eV as the exposure was increased to 0.84 L. The shift for the lower BE feature was larger than that for the higher BE feature (0.6 compared to 0.2 eV), and most of this difference occurred in the low exposure region. The larger downward BE shift for this atom relative to that of N atom in the middle suggests that at low coverage N_2O molecules are bound N-end-on at oxygen vacancy sites where charge transfer from the vacancy to N_2O may come into play. In contrast, the splitting between the two N 1s features of N_2O at higher coverages, where adsorption at non-defect sites should be more prevalent, resembled that observed for N_2O adsorbed on a variety of surfaces (see references in [5]). The existence of charge transfer from the vacancies to N_2O is also supported by electron energy loss data discussed below.

Monitoring the uptake of N_2O in XPS using the N 1s signal peak areas indicated that saturation of the signal at 105 K was achieved with exposures below 1 L (data not shown), which corresponds to a coverage of 3×10^{14} molecules/cm^2 with unity sticking. No other N 1s features were observed indicating that neither NO or atomic N were present in detectable amounts after N_2O adsorption at 105 K.

The upper trace in Fig. 7 shows the N 1s XPS spectra for a 0.84 L exposure at 105 K heated to 185 K. Based on the TPD data of Fig. 1, the surface should be void of any N-containing species after heating to this temperature. In agreement, XPS shows that virtually all of the N 1s signal was absent after heating to 185 K. However, a small N 1s signal was evident at 400.9 eV. Although this suggests that some N-related species were left on the surface after evolution of all desorption products, separate experiments (data not shown) involving prolonged exposure of adsorbed N_2O to X-rays indicates that X-ray damage was the cause of this 400.9 eV feature. This is consistent with results from Overbury et al. [5] who observed a weak N 1s peak at 400.5 eV from X-ray induced decomposition of N_2O adsorbed on CeO_2(1 1 1). They tentatively assigned this feature to N atoms because the binding energy did not match that of adsorbed nitrite, NO or nitride species.

3.3. Electron energy loss measurements

Electron energy loss measurements in the vibrational (HREELS) and electronic (EELS) ranges were conducted to provide additional insights into the chemistry of N_2O on TiO_2(1 1 0). In the vibrational regime, HREELS data suggest that the majority of the N_2O monolayer is relatively unperturbed in its adsorption on TiO_2(1 1 0). A saturation coverage at 90 K resulted in loss features at 2245 and 1240 cm^{-1} (data not shown) which are consistent with the ν(N=NO) and ν(NN=O) modes, respectively. These positions are similar to those of N_2O in the gas and condensed phases (see references in [9]). The resolution (60 cm^{-1}) and signal-to-noise (3:1) of the data did not provide confidence in distinguishing between Ti–NNO or Ti–ONN bonding, both of which have been observed on TiO_2 powder (see references in [9]). The poor quality of the HREELS data for a full monolayer of N_2O likely resulted from weak dynamic dipole intensities of adsorbed N_2O and not from N_2O molecules bound parallel to the surface (in which case neither of the N_2O modes would be dipole-allowed) since our uptake measurements suggest that at saturation there was a 1:1 ratio between N_2O and Ti^{4+} cation adsorption sites. Such a high coverage of N_2O would necessitate end-on bonding, as was observed for CO_2 [25], an isoelectronic analog of N_2O. All HREELS features attributable to N_2O were absent after heating the surface to 150 K (data not shown) in general agreement with the XPS data of Fig. 7.

In contrast to the insensitivity for N_2O in the vibrational region, electron energy loss measurements in the electronic regime (EELS) showed significant changes due to N_2O oxidation of vacancies. Fig. 8 shows EELS spectra for the clean TiO_2(1 1 0) surface possessing about 14% oxygen vacancy sites (upper trace), followed by increasing exposures of N_2O at 90 K. The spectral region in Fig. 8 was limited to 0–3 eV in order to accentuate the effect of N_2O on the vacancy-related loss feature at 0.8 eV. Intensity in the band-to-band loss region (>3 eV) increased with N_2O

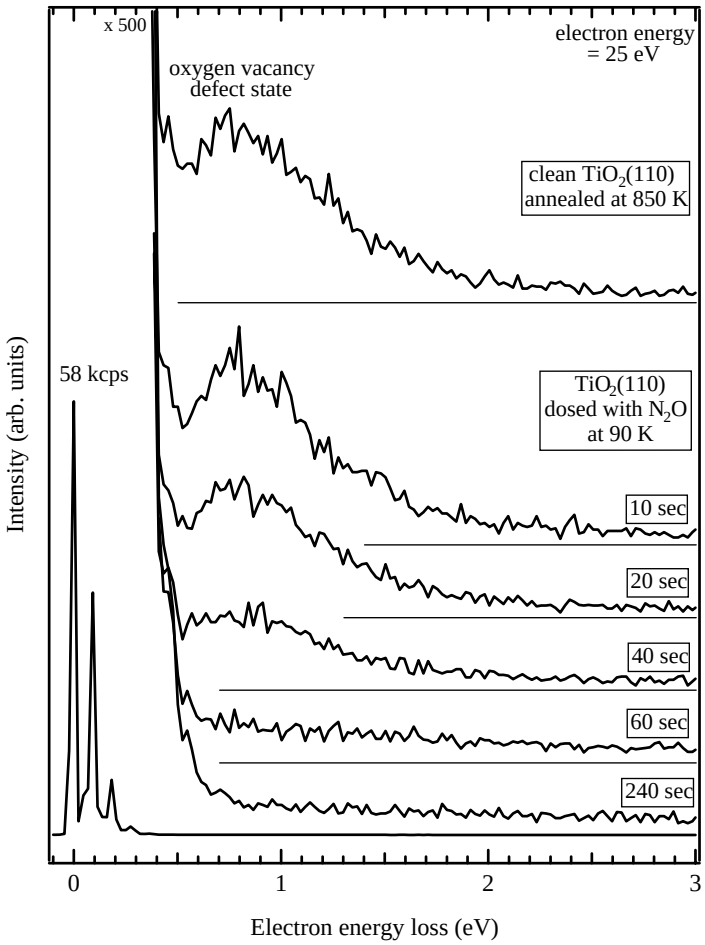

Fig. 8. EELS spectra from clean TiO_2(1 1 0) (upper trace), and from TiO_2(1 1 0) with increasing exposures of N_2O at 90 K. Spectra are displaced vertically for clarity, and representative baselines for each are shown as straight lines.

exposure, but no losses ascribable to molecularly adsorbed N_2O were detected. The doser used in these studies was not calibrated, however we estimate that saturation of the N_2O monolayer occurred at about a 180 s exposure based on changes in the elastic peak count rate. (The elastic peak, located at zero loss energy, is very sensitive to the degree of order on the surface. Intense losses between 0 and 0.4 eV were due to oxide phonon modes.) Data in Fig. 8 show that the most dramatic effect of N_2O adsorption at 90 K was the complete attenuation of the 0.8 eV feature. Virtually no change in the 0.8 eV feature occurred after a 10 s exposure, but the entire loss feature was absent after a 60 s exposure. Assuming that monolayer saturation was achieved after a 180 s exposure and that the sticking probability was essentially unity up to this exposure (as indicated by data in Fig. 4), then the vacancy feature was attenuated by less than 1/3 ML of N_2O. This coverage regime is in reasonably agreement with the XPS data of Fig. 7 which suggests charge transfer from vacancies to N_2O at the lowest coverages.

Fig. 9 shows EELS data that indicate the charge transfer from vacancies to N_2O is not reversible. As shown in the lower trace of Fig. 9, the vacancy loss feature at 0.8 eV was attenuated after a saturation exposure of N_2O at 90 K. This loss did not reappear after the surface was heated to 210 K, at which point TPD indicated the surface was free of adsorbed N_2O (see

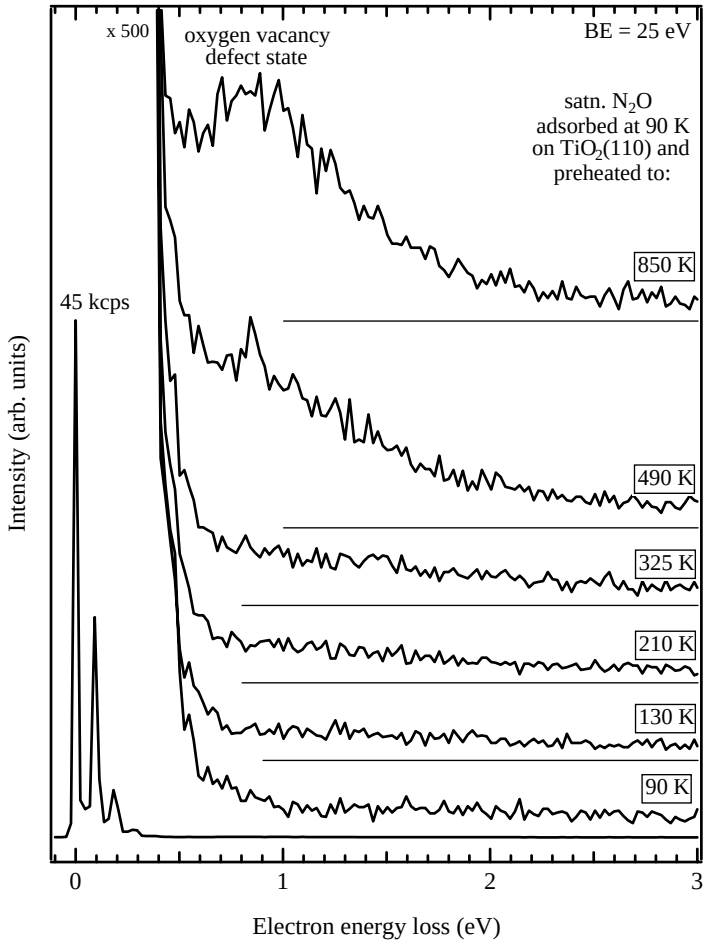

Fig. 9. EELS spectra from a saturation exposure of N_2O on TiO_2(1 1 0) at 90 K (lower trace) followed by heating to various temperatures. Spectra are displaced vertically for clarity, and representative baselines for each are shown as straight lines.

Fig. 1). The vacancy loss feature only appeared after heating the surface above about 450 K, in agreement with our previous studies of O_2-oxidized vacancies on TiO_2(1 1 0) [32]. This result, however, is in conflict with the TPD results of Fig. 5 which suggest that N_2O TPD to 250 K oxidized only about 50% of the vacancies present at adsorption. At present, we are unable to rationalize the contradiction between the TPD results of Fig. 5 and EELS results of Fig. 9. In contrast, Fig. 10 shows that N_2O exposed to TiO_2(1 1 0) at 310 K did not result in vacancy oxidation, in agreement with TPD data presented in Fig. 6. The N_2O exposure used in Fig. 10, when performed at 90 K, resulted in complete removal of the vacancy loss feature (lower trace), but the spectrum for an equivalent exposure at 310 K (middle trace) was essentially the same as that obtained after annealing the surface at 850 K (upper trace). This result confirms that the reactive sticking of N_2O significantly decreases above its desorption temperature.

4. Discussion

To briefly summarize the TPD and uptake results, we observe two channels of N_2O conversion to N_2 for N_2O dosed at 90 K on vacancy-defected TiO_2(1 1 0). One of these channels was observed at 90 K while

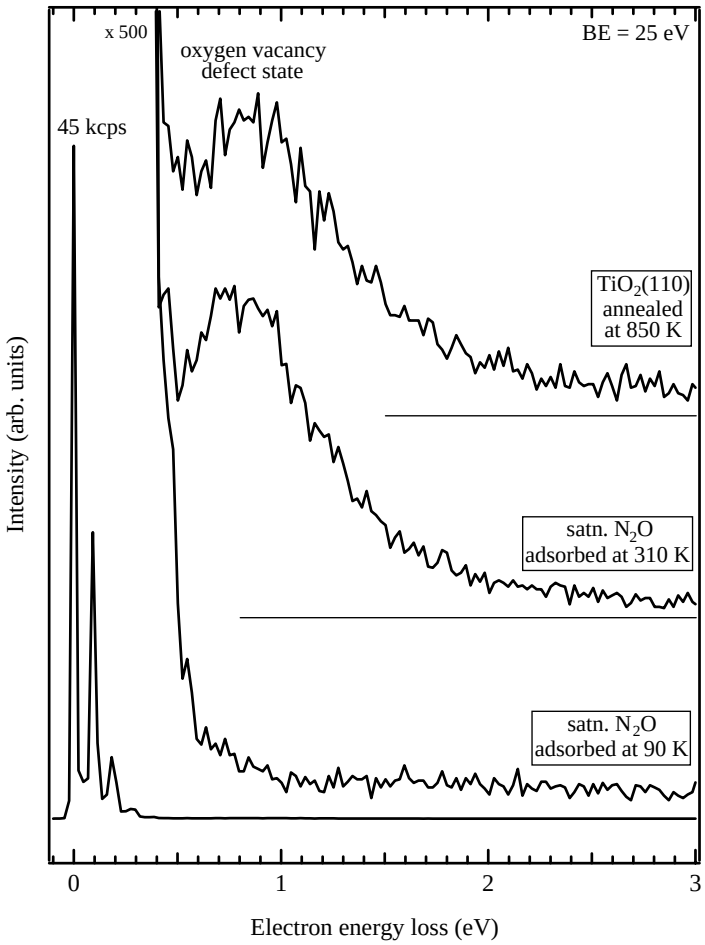

Fig. 10. EELS spectra from a saturation exposure of N_2O on TiO_2(1 1 0) at 90 K (lower trace) and at 310 K (middle trace), along with the spectrum for the clean surface (upper trace). Spectra are displaced vertically for clarity, and representative baselines for each are shown as straight lines.

dosing and the other occurred at 170 K during heating. These decomposition processes do not strongly compete with molecular N_2O adsorption and desorption based on the amount of N_2O observed in TPD. However, the levels of N_2 observed are consistent with vacancy-mediated processes. This is confirmed by changes in the surface induced by N_2O chemistry that becomes manifest in the 500 K vacancy-related water TPD state (see Fig. 6) as well as in the EELS data of Figs. 8–10.

A logical set of reactions that explain the oxidation of vacancies and the deposition of O adatoms are presented below. The reaction of N_2O to fill vacancies can be adequately described as

$$N_2O(g)+vac(2e^-) \rightarrow N_2(g)+O^{2-}\ (lattice) \quad (90\,K)$$

where 'vac($2e^-$)' refers to an oxygen vacancy site with two trapped electrons and 'O^{2-}(lattice)' refers to an oxidized vacancy. In this case, the overall effect could be reasonably argued to be from the addition of charge to the antibonding π-system of the N_2O molecule which destabilizes the NN=O bond leading to N_2 gas and a filled vacancy. We propose that this process involves N_2O bound at the vacancy O-end down, and that the N_2 emitted at 90 K comes from this process. In contrast to the lower temperature N_2

production process just described, we propose that the second reaction leading to N_2 formation at 170 K involves dissociation of N_2O at vacancy sites resulting in formation of oxygen adatoms according to

$$N_2O(g) + \text{vac}(2e^-) \rightarrow N_2O(\text{ads-vac}) \rightarrow N_2(g) + O(\text{adatom}) + \text{vac}(2e^-) \quad (170\,K)$$

In this case, the vacancy is not oxidized, but still catalyzes the dissociation of N_2O. As discussed below, we propose this pathway results from N_2O molecules that are bound at vacancies N-end down.

The feasibility of these processes depends on the ability of vacancies to transfer charge to adsorbed N_2O, which destabilizes the molecules π-system leading to decomposition. Several groups have shown that N_2O can function as an electron scavenger during photocatalysis over TiO_2 [2,3,7–10] resulting in reduction of this molecule. Similar arguments have been applied to the decomposition of other NO_x species at vacancy sites on TiO_2(1 1 0) [13,16,37]. The ability of adsorbed N_2O to accept charge is related to the molecule's electron affinity. McCarthy et al. [38] have noted that there is some disagreement about the stability of N_2O^-, with experimental and theoretical values for the electron affinity ranging from about 0.2 to −0.2 eV. These authors proposed that the stability of N_2O^- may depend on the ability of the ion to relax from a linear to bent geometry. Our results indicate that N_2O adsorbed at oxygen vacancies on TiO_2(1 1 0) readily accepts charge at 90 K, implying a positive electron affinity for adsorbed N_2O. Whether N_2O molecules adsorbed at vacancies adopt a bent or linear geometry is not discernable from our data, however Sorescu et al. [16,39] have proposed that a bent form of N_2O should be stable at vacancies on TiO_2(1 1 0). Using first-principles methods, these authors calculate that the binding energies of linear N_2O on TiO_2(1 1 0) are weak (below 10 kcal/mol for either N-down or O-down geometries), whereas the adsorption energy of a bent N_2O species that bridges an oxygen vacancy and a five-coordinate Ti^{4+} cation site exceeds 20 kcal/mol. Interestingly, the calculations of Sorescu et al. find that this bridge form of N_2O is more stable with the N-end bound at the vacancy and the O-end at the Ti^{4+} cation site. Such an adsorption geometry might explain the generation of O adatoms and the retention of vacancies after N_2O decomposition.

We therefore link the two channels of N_2 production from N_2O decomposition at oxygen vacancies to two conformers of N_2O adsorbed at vacancy sites. Sorescu et al. [16,39] have calculated that the O-down and N-down forms of linear N_2O are weakly bound, with the latter more stable than the former by about 4 kcal/mol. Both of these species have been observed on TiO_2 powder using infrared [9], along with analogs of each observed at minority sites that can be attributed to adsorption at electronic defects. The 1:1 ratio of vacancy filling to O adatom production seen in this study suggests that the stabilities of these two forms of N_2O at vacancies on TiO_2(1 1 0) are of equivalent strength. However, decomposition from either form is strongly dependent on the residence time in the respective adsorbed state based on our temperature-dependent studies.

5. Conclusions

Results in this study indicate that the reactivity of N_2O with TiO_2(1 1 0), especially with regards to N_2 formation, is dictated primarily by reactions at oxygen vacancy sites. In the presence of vacancies, N_2O decomposes through two channels, one that oxidizes vacancies and another that deposits oxygen adatoms on the surface. Both channels result in N_2 desorption, with one channel yielding gas phase N_2 on adsorption of N_2O at 90 K and the other yielding N_2 in TPD at 170 K. Based on comparisons with studies in the literature, we propose that the channel leading to vacancy oxidation results from the O-end down form of N_2O bound at vacancies and is responsible for the N_2 desorption observed during N_2O exposure at 90 K. The channel leading to oxygen adatom deposition and vacancy retention results from N-end down bonding of N_2O forming a stable bent form of N_2O. This species decomposes at 170 K to form O adatoms and gaseous N_2. Our results also show that both of these N_2O decomposition channels are strongly temperature-dependent under UHV conditions, with a reaction probability of $\leq 5 \times 10^{-4}$ at an adsorption temperature of 220 K. This implies that the conversion of N_2O to N_2 over clean TiO_2(1 1 0) requires both the presence of oxygen vacancy sites

and a sufficiently long residence time of N_2O at these vacancies.

Acknowledgements

This work was supported by the US Department of Energy, Office of Basic Energy Sciences, Divisions of Materials Sciences and Chemical Sciences. Pacific Northwest National Laboratory is a multiprogram national laboratory operated for the US Department of Energy by the Battelle Memorial Institute under Contract DE-AC06-76RLO 1830. The research reported here was performed in the William R. Wiley Environmental Molecular Science Laboratory, a Department of Energy user facility funded by the Office of Biological and Environmental Research.

References

[1] S.C. Christoforou, E.A. Efthimiadis, I.A. Vasalos, Catal. Lett. 79 (2002) 137.
[2] J. Cunningham, A.L. Penny, J. Phys. Chem. 78 (1974) 870.
[3] J. Cunningham, D.J. Morrissey, E.L. Goold, J. Catal. 53 (1978) 68.
[4] A. Boronicolos, J.C. Vickerman, J. Catal. 100 (1986) 59.
[5] S.H. Overbury, D.R. Mullins, D.R. Huntley, L. Kundakovic, J. Catal. 186 (1999) 296.
[6] G. Busca, V. Lorenzelli, J. Catal. 72 (1981) 303.
[7] M. Anpo, N. Aikawa, Y. Kubokawa, M. Che, C. Louis, E. Giamello, J. Phys. Chem. 89 (1985) 5017.
[8] A. Kudo, H. Nagayoshi, Catal. Lett. 52 (1998) 109.
[9] C.N. Rusu, J.T. Yates Jr., J. Phys. Chem. B 105 (2001) 2596.
[10] Y. Onishi, Bull. Chem. Soc. Jpn. 45 (1972) 922.
[11] U. Diebold, Surf. Sci. Rep. 48 (2003) 53.
[12] H. Courbon, P. Pichat, J. Chem. Soc., Faraday Trans. 1 80 (1984) 3175.
[13] G. Lu, A. Linsebigler, J.T. Yates Jr., J. Phys. Chem. 98 (1994) 11733.
[14] S. Hu, T.M. Apple, J. Catal. 158 (1996) 199.
[15] H. Yamashita, Y. Ichihashi, S.G. Zhang, Y. Matsumura, Y. Souma, T. Tatsumi, M. Anpo, Appl. Surf. Sci. 121–122 (1997) 305.
[16] D.C. Sorescu, C.N. Rusu, J.T. Yates Jr., J. Phys. Chem. B 104 (2000) 4408.
[17] M. Takeuchi, H. Yamashita, M. Matsuoka, M. Anpo, T. Hirao, N. Itoh, N. Iwamoto, Catal. Lett. 66 (2000) 185.
[18] C.N. Rusu, J.T. Yates Jr., J. Phys. Chem. B 104 (2000) 1729.
[19] G.S. Herman, C.H.F. Peden, J. Vac. Sci. Technol. A 12 (1994) 2087.
[20] M.A. Henderson, Surf. Sci. 355 (1996) 151.
[21] M.A. Henderson, W.S. Epling, C.H.F. Peden, C.L. Perkins, J. Phys. Chem. B 107 (2003) 534.
[22] J. Grimblot, P. Alnot, R.J. Behm, C.R. Brundle, J. Electr. Spectrosc. Relat. Phenom. 52 (1990) 175.
[23] S. Haq, A. Hodgson, Surf. Sci. 463 (2000) 1.
[24] A. Linsebigler, G. Lu, J.T. Yates Jr., J. Chem. Phys. 103 (1995) 9438.
[25] M.A. Henderson, Surf. Sci. 400 (1998) 203.
[26] D.A. King, M.G. Wells, Surf. Sci. 29 (1972) 454.
[27] R.K. Brown, D.A. Sharma, W.A. King, S. Haq, J. Phys. Chem. 100 (1996) 12559.
[28] A.N. Shultz, W.M. Hetherington III, D.R. Baer, L.-Q. Wang, M.H. Engelhard, Surf. Sci. 392 (1997) 1.
[29] M.A. Henderson, Surf. Sci. Rep. 46 (2002) 1.
[30] M.B. Hugenschmidt, L. Gamble, C.T. Campbell, Surf. Sci. 302 (1994) 329.
[31] D. Brinkley, M. Dietrich, T. Engel, P. Farrall, G. Gantner, A. Schafer, A. Szuchmacher, Surf. Sci. 395 (1998) 292.
[32] W.S. Epling, C.H.F. Peden, M.A. Henderson, U. Diebold, Surf. Sci. 412/413 (1998) 333.
[33] M.A. Henderson, S. Otero-Tapia, M.E. Castro, Faraday Discuss. 114 (1999) 313.
[34] R. Schaub, E. Wahlström, A. Ronnau, E. Laegsgaard, I. Stensgaard, F. Besenbacher, Science 299 (2001) 377.
[35] M.A. Henderson, W.S. Epling, C.L. Perkins, C.H.F. Peden, U. Diebold, J. Phys. Chem. B 103 (1999) 5328.
[36] D.R. Lide (Ed.), Handbook of Chemistry and Physics, CRC Press, New York, 2001.
[37] J.A. Rodriguez, T. Jirsak, G. Liu, J. Hrbek, J. Dvorak, A. Maiti, J. Am. Chem. Soc. 123 (2001) 9597.
[38] M.C. McCarthy, J.W.R. Allington, K.O. Sullivan, Mol. Phys. 96 (1999) 1735.
[39] D.C. Sorescu, J.T. Yates Jr., J. Phys. Chem. B 106 (2002) 6184.